

Optical trap detector for calibration of optical fiber powermeters: coupling efficiency

John H. Lehman and Christopher L. Cromer

The optical trap detector is based on two, 1 cm \times 1 cm silicon photodiodes and a spherical mirror contained in a package that is highly efficient for measuring light diverging from the end of an optical fiber. The mathematical derivation of the coupling efficiency relies on the integral directional response weighted by the angular intensity distribution of an idealized parabolic optical beam. Results of directional-uniformity measurements, acquired with the aid of a six-axis industrial robotic arm, indicate that the trap has a collection efficiency greater than 99.9% for a fiber numerical aperture of 0.24. Spatial uniformity measurements indicate that the variation of detector response as a function of position is less than 0.1%. The detector's absolute responsivity at 672.3, 851.7, and 986.1 nm is also documented by comparison with other optical detectors and various input conditions and indicates that the design is well suited for laser and optical fiber power measurements.

OCIS codes: 060.2380, 120.3930.

1. Introduction

The demand for laser and optical fiber powermeter (OFPM) calibrations has increased along with the proliferation of optical communications systems. As these systems become more sophisticated and the market for such equipment becomes increasingly competitive, the need for measurements having lower uncertainty is urgent. The accurate calibration of OFPMs is made difficult by the limited field of view of primary standards for laser power (devices that compare absorbed optical power to dissipated electrical power) and because of most available transfer standards. The measurement uncertainty associated with the coupling of the diverging radiation from the optical fiber and the OFPM are typically a major contribution to the total uncertainty of an OFPM calibration. This uncertainty often exceeds 1%, and is substantially greater than the uncertainty of the primary standards used with collimated beams.¹

In this paper we describe our efforts to provide lower uncertainty for OFPM calibrations through the development of a transfer standard with a coupling efficiency very near unity for optical fiber with a nu-

merical aperture (NA) of as much as 0.26; this accommodates measurements with most optical fiber presently used in optical communications. The transfer standard can thus be calibrated directly against a primary standard with collimated radiation and used to measure optical power from a fiber accurately, without intervening optics.

The detector described here makes use of two detecting elements and a spherical mirror to achieve a high coupling efficiency over broad angles. We have implemented it initially with silicon (Si) photodiodes, which cover the important 800- to 900- and 980-nm spectral regions. They are, however, suitable for use in calibrating instruments over the broader range of 450 to 990 nm, which is supported by some commercial OFPMs. The same design has been used with either germanium (Ge) or indium gallium arsenide (InGaAs) photodiodes to extend its range to 1800 nm.

2. Design Description

The trap detector is based on two Si photodiodes 10 mm \times 10 mm square and a silver-coated concave mirror (40-mm focal length, 15-mm diameter). The photodiodes and mirror are placed in a hardware fixture having a threaded aperture suitable for an optical fiber connector. This design is similar to a previously documented Ge-photodiode and mirror-trap design.² Unlike in the previous design, the diodes are mounted on a ceramic carrier, with electrical-contact pads in the same plane. This mounting allows the diodes to be placed closer to-

The authors are with the National Institute of Standards and Technology 81501, Sources and Detectors Group, 325 Broadway, Boulder, Colorado 80305. J. H. Lehman's e-mail address is lehman@boulder.nist.gov.

Received 20 February 2002; revised manuscript received 11 July 2002.

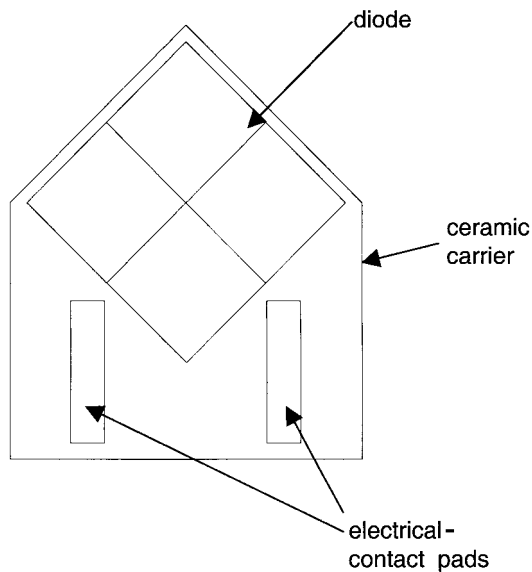


Fig. 1. Plan view of the diode mounted on a five-sided ceramic carrier with electrical-contact pads.

gether and closer to the input aperture. A schematic of a single diode mounted on the ceramic carrier is shown in Fig. 1. The relation of the five-sided carrier and the position of the diodes (with the mirror removed) is shown in Fig. 2.

Shown in Fig. 3 are the orientation of the photodiodes and the mirror, along with a geometric representation of light diverging from the center of the aperture as from the end of an optical fiber. Each photodiode is oriented relative to the aperture so that the principal ray intersects each diode once in sequence at a 45° angle of incidence, and after reflecting from the concave mirror, the ray intersects back

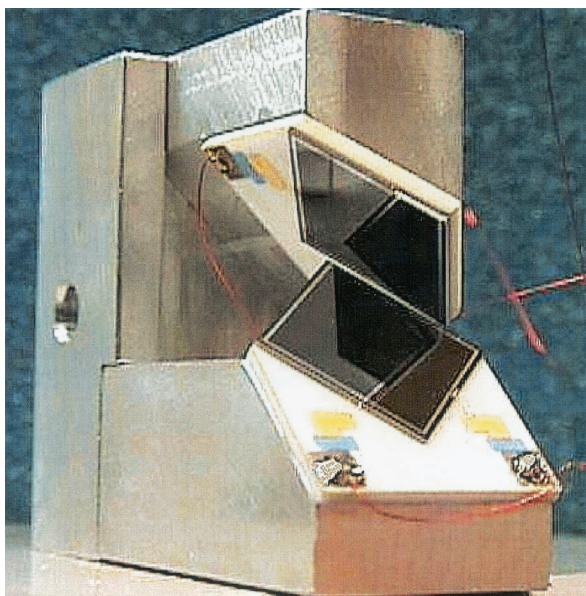


Fig. 2. Two Si photodiodes mounted relative to each other (mirror and aperture-bearing case removed).

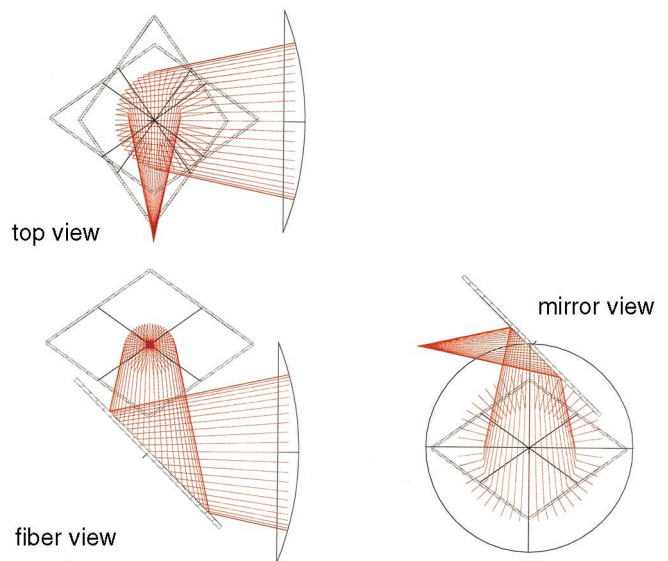


Fig. 3. Relative orientation of the photodiodes, concave mirror, and diverging input beam depicted in three views.

again in reverse order. The concave-mirror curvature was selected and the mirror surface positioned so that the path of the reflected beam is nearly identical to that of the incoming beam (which has a 28° divergence angle). A collimated beam, after being reflected by the concave mirror, has a focal plane located between the fourth and the fifth reflections (the beam converges before exiting the trap cavity).

3. Robotic Arm and Measurement Apparatus

The measurements of the field of view and spatial uniformity were accomplished with the aid of a six-axis, industrial (commercially available) robot arm having six degrees of freedom, with optical encoders providing position information on each axis. The manufacturer has specified that the robotic arm is capable of positioning the robot's wrist with a precision of $10 \mu\text{m}$ in terms of orthogonal coordinates x , y , and z and with a rotation precision of 0.01° in terms of angular coordinates α , β , and γ . For convenience, we refer to these coordinates (x , y , z , α , β , and γ) as robot coordinates. In principle, robot coordinates refer to spherical coordinates relative to some arbitrary point in space that is fixed relative to the robot and coincident with the center of the aperture of the detector being evaluated. These coordinates, shown in Fig. 4, are useful for mapping the normalized intensity profile (discussed later) in coordinates that are consistent with the measurement results for the detector's directional responsivity.

The robotic arm was used to position a temperature-stabilized, 850-nm wavelength laser diode. The laser diode was attached to the robot's wrist so that the beam axis was coaxial with the wrist rotation, defined by robot coordinate γ . The diode laser was focused at coordinates $x = 0$, $y = 0$, and $z = 0$, with a 100-mm focal-length lens, and to a beam

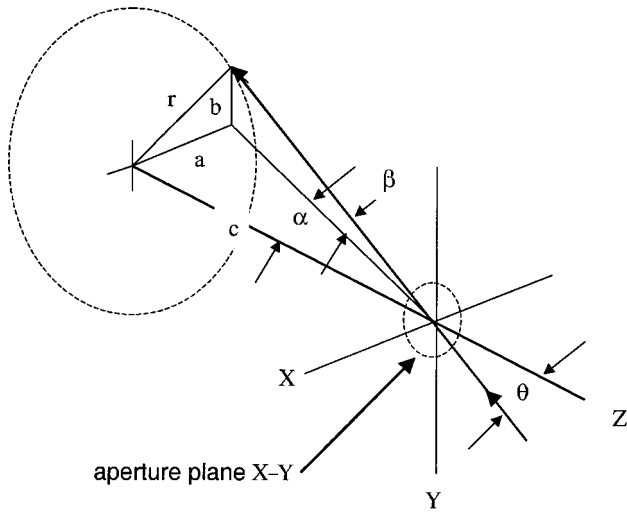


Fig. 4. Geometric relation of the robot's coordinates, the detector's aperture plane, and the orientation of the angle of incidence of the probe beam at angle θ .

diameter of approximately 0.1 mm (that is, 99.9% of the total beam power was within a radius of 0.05 mm of the beam's centroid). For each measurement, the focal point and the optical axis of the probe beam were initially aligned to be centered and normal to the detector-aperture plane. The absolute positioning accuracy was approximately three times the value of the precision stated by the manufacturer. Using the spatial response of a lithographically patterned pyroelectric detector as a resolution target, we have determined that the positioning uncertainty is within the stated accuracy of 30 μm and 0.03°.

During each field-of-view measurement the laser was incrementally rotated by an angle α away from normal incidence. Then the laser was incrementally rotated by angle β , for each angle α , to define the probe beam's orientation relative to the center of the detector aperture. At each increment, the detector's response was sampled, and the variation relative to the response at normal incidence was recorded. The essential data from the measurement were the incremental position of (α, β) and the detector's current response at each increment.

For each spatial uniformity measurement, the laser was incrementally positioned in a two-dimensional plane defined by $z = 0$, $\alpha = 0$, and $\beta = 0$. For each position in the plane, the detector's current response was sampled and recorded.

4. Beam-Profile Formulation

To evaluate the detector design, we have estimated the uncertainty for a given optical fiber using a mathematical model of the beam's intensity profile based on the NA of the optical fiber. The intensity profile was translated into robot coordinates and mapped onto the directional-uniformity measurements of the detector to determine the overall coupling efficiency.

The far-field intensity distribution of laser light emitted from a multimode fiber is principally a func-

tion of the fiber NA, the launching conditions at the input, and the length of fiber. The far-field divergence from multimode telecommunications fiber greatly exceeds that of single-mode fiber. For that reason we consider the output of a multimode fiber as an example of the largest divergence likely to be encountered by an OFPM.

Regardless of the wavelength and the fiber chosen, the divergence of light from the exit end of the fiber is less than the angle defined by the NA of the fiber. Multimode, graded-index communication fiber typically has a range of NA between 0.20 and 0.28, which corresponds to a maximum full divergence angle $2\theta_w$ of approximately 32°. The NA is related to θ_w by

$$\text{NA} = \sin(\theta_w). \quad (1)$$

We have used an approximation to a strictly parabolic intensity distribution, which is

$$P(r) = \frac{1 - [r/r_w]^2}{1 - [r/r_w]^{40}}, \quad (2)$$

where

$$r = c \tan(\theta), \quad (3)$$

$$r_w = c \tan(\theta_w). \quad (4)$$

The value of r is a distance from the optical axis defined by incidence angle θ and a distance c beyond the aperture plane. The beam's half-width r_w is defined for a specified divergence half-angle θ_w [from Eq. (1)]. This profile matches the generally observed output distribution of a multimode fiber with a quadratic behavior near the center of the distribution and a small tail near the maximum divergence half-angle. This equation is based on the criterion of defining the beam width r_w as equal to the beam diameter where the irradiance is 5% of the irradiance at the center ($r = 0$). (The choice of the 5% level is based on the recommendation of the Telecommunication Industry Association in the United States, and others, for determining the NA of an optical fiber.³)

To evaluate the detector's coupling efficiency, we must incorporate the detector's measured directional response $R(\alpha, \beta)$ as a function of angle of incidence, relative to the center of the X-Y plane of the detector aperture. The position (α, β) is related to the angle of incidence θ by the equation

$$\cos(\theta) = \cos(\alpha)\cos(\beta). \quad (5)$$

An example of the normalized intensity profile for $2\theta_w = 4^\circ (\pm 2^\circ)$, $20^\circ (\pm 10^\circ)$, and $32^\circ (\pm 16^\circ)$ is shown in Fig. 5.

In principle, the collection efficiency, η , of the trap detector is a convolutionlike integral of the calculated beam profile $P(\alpha, \beta)$ and the measured, relative directional response $R(\alpha, \beta)$ of the detector for a finite

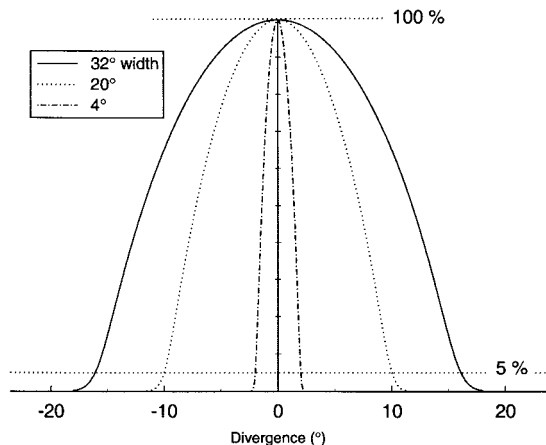


Fig. 5. Sample profiles of the normalized beam irradiance at $\pm 2^\circ$, $\pm 10^\circ$, and $\pm 16^\circ$.

beam divergence ($2\theta_w$) and the entire, field of view of the detector:

$$\eta = \int_{-\pi/2}^{\pi/2} \int_{-\pi/2}^{\pi/2} \left[\frac{P(\alpha, \beta) R(\alpha, \beta)}{\cos(\alpha) \cos^2(\theta)} \right] d\alpha d\beta. \quad (6)$$

In Eq. (6), it is assumed that the detector's response $R(\alpha, \beta) = 1$ at $(\alpha, \beta) = (0, 0)$ and that the beam profile is normalized so that

$$1 = \int_{-\pi/2}^{\pi/2} \int_{-\pi/2}^{\pi/2} \left[\frac{P(\alpha, \beta)}{\cos(\alpha) \cos^2(\theta)} \right] d\alpha d\beta. \quad (7)$$

In practice, evaluation of the coupling efficiency is limited because one has a finite data set that is acquired when the detector's response is sampled at incremental positions of the robotic arm, thus satisfying a two-dimensional array of positions. For the detector's response $R(\alpha, \beta)$ at each robotic arm position θ , we calculated a value of the normalized intensity profile $P(\alpha, \beta)$.

5. Directional Uniformity and Coupling Efficiency

We acquired $R(\alpha, \beta)$ and calculated $P(\alpha, \beta)$ for values of α and β ranging from 0° to $\pm 16^\circ$ at 2° increments (maximum $\theta = 22.5^\circ$). The measurement results of $R(\alpha, \beta)$ are shown in Fig. 6, with the relative detector response as ordinate values and with the angle of incidence θ as abscissa values. Several values of $R(\alpha, \beta)$ for a single value of θ are apparent in Fig. 6 because the value of θ is the same for unique pairs of $\pm\alpha$ and $\pm\beta$, directed in each quadrant of the X - Y plane. Figure 7 shows the relative coupling efficiency as a function of NA calculated from Eq. (6), where the NA is related to θ_w as shown in Eq. (1). Each data point corresponds to incremental values of the normalized intensity profile (three examples of which are shown in Fig. 5). The coupling efficiency is a quantitative basis for expressing the uncertainty of the directional-uniformity measurements shown in Fig. 6. The uncertainty can be stated for any NA that we wish to define as long we assume that the

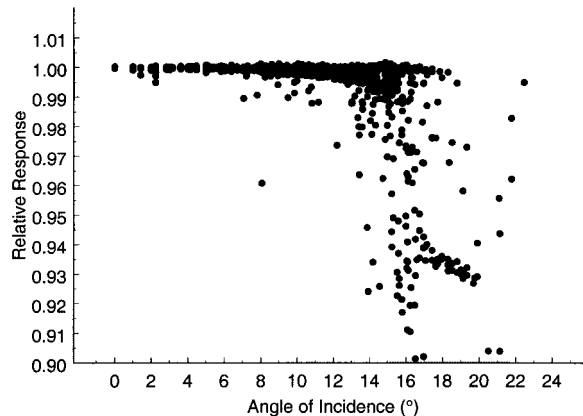


Fig. 6. Directional responsivity measurement results.

parabolic intensity profile is a reasonable worst-case situation for light leaving a fiber and entering the detector. The results shown in Fig. 7 indicate that the coupling efficiency of the trap detector is greater than 99.9% for NA values of as much as 0.24 ($\pm 14^\circ$ fiber-exit divergence) and 99.5% for subsequent NA values of as much as 0.28 ($\pm 16^\circ$ fiber-exit divergence). The coupling efficiency loss is therefore between 0.1% and 0.5% for an NA between 0.24 and 0.28, which may be associated with the extreme range of the expected divergence from multimode communication fiber (core diameter of 50 or $62.5 \mu\text{m}$ and transmitting laser light in the visible and in the near infrared). Therefore, for multimode fiber-coupled measurements of absolute responsivity it is reasonable to incorporate a type B uncertainty of 0.1% to 0.5% into the overall measurement uncertainty of which the detector is capable.⁴

6. Spatial Uniformity

Evaluation of the detector's spatial uniformity is particularly important when we compare differences between fiber-coupled and free-space laser measurements. In the case of fiber-coupled mea-

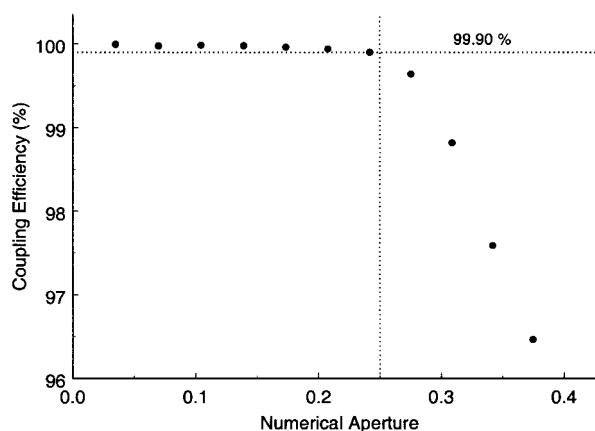


Fig. 7. Coupling efficiency η of the optical trap detector determined from the normalized beam profile and measurement results shown in Fig. 6.

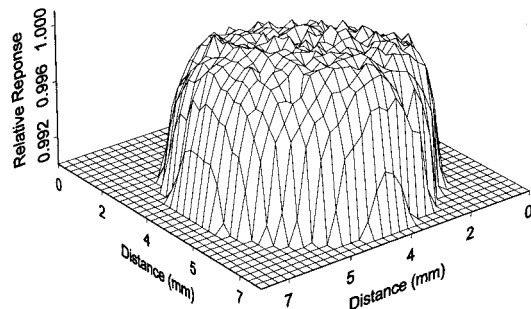


Fig. 8. Spatial uniformity of the Si trap detector.

measurements, the position of an incoming beam is fixed relative to the fiber connector, which is rigidly attached to the detector. The position and size of an incoming free-space laser beam may vary. If the detector's response is not uniform as a function of the position, then all other things being equal between the fiber and the free-space measurement, the uncertainty of the measurement depends on the variation of the detector's response as a function of position.

We measured the detector's spatial uniformity using a laser mounted on the robotic arm as described in Section 3. The laser beam was scanned at 0.5-mm intervals across a 10 mm \times 10 mm planar area and centered on the detector aperture (normal to the detector aperture and at a 45° angle of incidence relative to the first photodiode surface) while the detector output data were collected. The results shown in Fig. 8 indicate that the responsivity varies by less than 0.1% over a 7 mm \times 7 mm area centered on the detector aperture. This variation is significantly less than that of our existing transfer standard for OFPM calibrations for the 450- to 1100-nm wavelength range.⁵ Based on this variation, we must incorporate a type B uncertainty of 0.1%.

We have addressed the properties of spatial and of directional uniformity, and hence the relative coupling efficiency, because they represent an evaluation of the aspects of the detector design that are new and unique. The absolute responsivity is also important from the standpoint of comparing the detector's performance for fiber-coupled versus free-space measurements and represents the necessary and intended use of the transfer standard over a range of wavelengths and optical input conditions. In other words, the outcome of the absolute responsivity com-

parisons tells us whether the transfer standard can do the work for which it was designed.

7. Absolute Responsivity

We measured the absolute responsivity using three different comparison methods. The responsivity was compared with a wedge-trap pyroelectric detector over a range of wavelengths from 450 to 1100 nm, at 10-nm increments by means of a monochromator and a broadband-lamp source.¹ The responsivity was also compared with that of an electrically calibrated pyroelectric detector at discrete laser wavelengths in two different ways. In one case the light was transmitted by fiber and connected to the detector aperture with an FC-type connector, and in the other case the light was nearly collimated and transmitted through space. In the latter two comparisons, the calibration traceability and uncertainty have been documented and discussed by Vayshenker *et al.*⁶ By finding agreement in the absolute responsivity measured three different ways, we have further evidence that the detector is highly efficient and that the measurement uncertainty we assess on the basis of directional and spatial uniformity measurements is reasonable.

The results of the absolute responsivity measurements are shown in Table 1. Using collimated laser beams at 672.3, 851.7, and 986.1 nm, we found that the absolute spectral responsivity was nearly the same as that measured with a lamp source and a monochromator. With the same laser sources, but with the radiation transmitted through fibers terminated with FC/PC-type connectors, the absolute responsivity at each wavelength was nearly identical to that obtained when collimated beams or a lamp source was used. The expanded uncertainty (with an expansion factor of $k = 2$) of the lamp and the monochromator measurements was less than 1.25%, and less than 0.5% for the laser-based measurements.

8. Comparison

The maximum difference in absolute responsivity between open-beam and fiber-coupled measurement results, determined from the calibration of laser powermeters at our facility, has been as large as 10%.⁷ The 0.1% difference (fifth column, Table 1) measured for the current device demonstrates that the large uncertainties of absolute responsivity ob-

Table 1. Absolute Spectral Responsivity

Wavelength (nm)	Laser Collimated (A/W)	Laser FC/PC Fiber Connector (A/W)	Lamp Monochromator (f/4) (A/W)	Difference (%) ^a
672.3	0.5389	0.5370	0.5376	-0.11
851.7	0.6804	0.6815	0.6810	-0.07
986.1	0.7770	0.7770	0.7766	0.05

^aDifferences from laser FC/PC fiber connector and lamp monochromator.

tained in the past depend on the test detector and not on the measurement system. This fact does not mean that the laser powermeters we have calibrated in the past are unsuitable for optical fiber power measurements. Rather, if fiber-coupled absolute responsivity measurements are to be compared with open-beam absolute responsivity measurements (that is, without fiber attached to a fiber connector), some detector designs are better suited than others.

9. Discussion

The trap design has been adapted to Ge as well as to InGaAs photodiodes for measurements at longer wavelengths, such as between 850 and 1750 nm. In principle, Ge or InGaAs photodiodes in the trap configuration are as equally well suited at longer wavelengths as the Si photodiodes are for shorter wavelengths. It may be argued, however, that InGaAs photodiodes are preferred over Ge photodiodes because InGaAs photodiodes have higher quantum efficiency at room temperature and are less sensitive to ambient temperature variations.⁸ Unfortunately, spatially uniform InGaAs photodiodes, if available, are nearly ten times more expensive than Ge photodiodes.⁹ Also, as with the use of any large-area photodiodes (or several small photodiodes electrically connected in parallel), one must know the shunt resistance when using large Ge or InGaAs photodiodes. Unacceptably low shunt resistance may prevent accurate evaluation of small optical signals that are common for optical fiber power measurements.¹⁰ The problem of low shunt resistance can be addressed by use of a current-to-voltage converter for each photodiode in the trap or by use of an amplifier designed to accommodate the low shunt resistance, but this complicates the design and introduces other trade-offs.⁸

10. Conclusion

The feature that distinguishes this trap detector from its predecessors is its uniform directional responsivity over a larger acceptance angle. Our goal in performing this evaluation was to state an uncertainty contribution based on the quantitative evaluation of the coupling efficiency rather than on estimates used in the past. Our measurement results indicate that the detector is well suited for input from collimated laser sources as well as from multimode fiber having

an NA as large as 0.26. The benefits of high optical-to-electrical conversion efficiency, reasonable cost, and excellent directional and spatial uniformity make the detector a valuable tool for calibrating laser and OFPMs.

We thank Igor Vayshenker for the optical fiber power measurements and the Calibration Coordination Group (by direction of the U.S. Navy and the U.S. Army Standards Laboratories) for support of this research.

References

1. J. H. Lehman, "Calibration service for spectral responsivity of laser and optical-fiber power meters at wavelengths between 0.4 μm and 1.8 μm ," NIST Spec. Publ. 250-53 (National Institute of Standards and Technology, Boulder, Colo., 1999), pp. 1–39.
2. J. H. Lehman and X. Li, "A transfer standard for optical fiber power metrology," *Eng. Lab. Notes in Opt. & Photon. News*, May 1999 [Appl. Opt. **38**, pp. 7164–7166 (1999)].
3. E. M. Kim and D. L. Franzen, "Measurement of far field radiation patterns from optical fibers," *Nat. Bur. Stand (U.S.) Spec. Publ. 637* (National Institute of Standards and Technology, Boulder, Colo., 1983), Vol. 2, pp. 187–206.
4. B. N. Taylor and C. E. Kuyatt, "Guidelines for evaluating and expressing the uncertainty of NIST measurement results, NIST Technical Note 1297 (National Institute of Standards and Technology, Boulder, Colo., 1994), p. 2.
5. C. A. Hamilton, G. W. Day, and R. J. Phelan, "An electrically calibrated pyroelectric radiometer system," *Nat. Bur. Stand (U.S.) Technical Note 678* (National Institute of Standards and Technology, Boulder, Colo., 1976).
6. I. Vayshenker, X. Li, D. J. Livigni, T. R. Scott, and C. L. Cromer, "NIST measurement services: optical fiber power meter calibrations at NIST," NIST Spec. Publ. 250-54 (National Institute of Standards and Technology, Boulder, Colo., 1999) pp. 1–36.
7. R. L. Gallawa and X. Li, "Calibration of optical fiber power meters: the effect of connectors," *Appl. Opt.* **26**, 1170–1174 (1987).
8. G. Eppeldauer, "Optical radiation measurement with selected detectors and matched electronic circuits between 200 nm and 20 μm ," NIST Technical Note 1438 (National Institute of Standards and Technology, Boulder, Colo., 2001), pp. 63–68.
9. E. Theocharous, N. P. Fox, and T. R. Prior, "A comparison of the performance of infrared detectors for radiometric applications," in *Optical Radiation Measurements III*, J. M. Palmer, ed., *Proc. SPIE* **2815**, 56–68 (1996).
10. N. P. Fox, "Improved near-infrared detectors," *Metrologia* **30**, 321–325 (1993).